water

MDPI

Article

From Waste to Biosorbent: Removal of Congo Red from Water by Waste Wood Biomass

Marija Stjepanović [1], Natalija Velić [1,*], Antonela Galić [1], Indira Kosović [1], Tamara Jakovljević [2] and Mirna Habuda-Stanić [1]

[1] Faculty of Food Technology Osijek, University of Osijek, F. Kuhača 20, 31000 Osijek, Croatia; marija.stjepanovic@ptfos.hr (M.S.); agalic@ptfos.hr (A.G.); indira.kosovic@ptfos.hr (I.K.); mirna.habuda-stanic@ptfos.hr (M.H.-S.)

[2] Croatian Forest Research Institute, Cvjetno Naselje 41, 10450 Jastrebarsko, Croatia; tamaraj@sumins.hr

* Correspondence: natalija.velic@ptfos.hr

Abstract: The aim of the study was to screen the waste wood biomass of 10 wood species as biosorbents for synthetic dye Congo Red (CR) removal from water and to single out the most efficient species for further batch biosorption experiments. Euroamerican poplar (EP), the most efficient species achieving 71.8% CR removal and biosorption capacity of 3.3 mg g^{-1}, was characterized by field emission scanning electron microscopy (FE-SEM) and Fourier transform infrared spectroscopy (FTIR). Different factors affecting the biosorption process were investigated: initial biosorbent concentration (1–10 g dm^{-3}), contact time (5–360 min), initial CR concentration (10–100 mg dm^{-3}), and the initial pH (pH = 4–9). The results showed that CR removal efficiency increased with the increase of biosorbent concentration and contact time. Increase of initial CR concentration led to an increase of the biosorption capacity, but also a decrease of CR removal efficiency. The highest CR removal efficiency was achieved at pH = 4, while at pH = 9 a significant decrease was noticed. The percentage of CR removal from synthetic wastewater was 18.6% higher than from model CR solution. The Langmuir model fitted well the biosorption data, with the maximum biosorption capacity of 8 mg g^{-1}. The kinetics data were found to conform to the pseudo-second-order kinetics model.

Keywords: biosorption; biosorbent; Congo Red; waste wood biomass; wastewater

Citation: Stjepanović, M.; Velić, N.; Galić, A.; Kosović, I.; Jakovljević, T.; Habuda-Stanić, M. From Waste to Biosorbent: Removal of Congo Red from Water by Waste Wood Biomass. *Water* **2021**, *13*, 279. https://doi.org/10.3390/w13030279

Academic Editor: Hans Brix
Received: 22 December 2020
Accepted: 21 January 2021
Published: 24 January 2021

1. Introduction

The use of waste materials for different purposes has been widely promoted through the implementation of circular economy principles in the developmental strategies of many countries. Waste wood biomass, generated in substantial amounts by wood and wood processing industries, has mostly been further exploited for heat and power, thus replacing non-renewable energy sources (e.g., coal or natural gas) with a renewable, more sustainable one [1]. However, a large portion of waste wood biomass remains unexploited, therefore posing a possible environmental danger.

Another serious environmental problem is the presence of synthetic dyes in aquatic ecosystems. Synthetic dyes have been irreplaceable in almost every industry and are often present in industrial effluents. The discharge of poorly treated or untreated dye-loaded industrial effluents into the natural recipients (i.e., the aquatic ecosystem) significantly affects the physical and chemical properties of their water [2]. Furthermore, even a minimal concentration of dyes can adversely affect the flora and fauna of the natural recipient. Many synthetic dyes have been reported as toxic, mutagenic, or carcinogenic [3,4]. Given the complex chemical structures and the application requirements for dyes, they show stability to heat, light, and oxidation and recalcitrance towards microbial degradation [2]. The efficiency of conventional biological wastewater treatment systems for dye removal is usually very low [5], which results in their accumulation and persistence in the environment.

Numerous methods (physical, chemical, and biological) for synthetic dye removal from water have been studied and developed. However, adsorption is still the most commonly used method, especially on a large-scale [6], because of its versatility, ease of use, and efficiency. Activated carbon, the most frequently used adsorbent for dye removal, efficiently removes cationic, mordant, and acid dyes, while its efficiency for dispersed, direct, vat, and reactive dyes is slightly lower [2]. Often the main drawback of commercially available activated carbons is their price and problems with regeneration, i.e., regeneration is not straightforward and may result in reduced adsorption capacity [6]. Furthermore, the problem with widely used coal-based commercial activated carbons (that efficiently remove a whole range of water pollutants) is that coal itself is a fossil fuel and therefore a non-renewable resource which soon might cease to exist. Therefore, many other materials (especially lignocellulosic waste materials), are being investigated as possible low-cost adsorbents for dye removal, either in their native (unmodified) or modified form (including the biochar form). Being relatively cheap, widely available during the whole year, and requiring little or no processing, waste wood biomass meets the conditions to be considered a low-cost adsorbent. Furthermore, since it is a biological (organic) material, it can be classified as a biosorbent. Biosorption is an adsorption subcategory, with the adsorbent being of biological origin [7]. Wood biomass is composed primarily of three polymers: cellulose (40–45% of the wood's dry weight), hemicellulose (30% of the wood's dry weight), and lignin (20–30%) [8]. The adsorptive removal of dyes (and other contaminants) from water is mainly accomplished by the interaction of dyes and specific functional groups of lignocellulosic polymers (e.g., -OH and -COOH). Table 1 gives the examples of waste wood biomass of different locally available wood species that have been evaluated as biosorbents for synthetic dyes' removal from water, including anionic azo dye Congo Red (CR), a model dye used in this study.

Table 1. Removal of synthetic dyes using waste wood biomass as biosorbent.

Dye	Biosorbent	q_{max}/mg g^{-1} (Langmuir)	% Removal	Ref.
Congo Red	Pine bark	1.6	100	[9]
	Lemon-scented gum sawdust	0.523	>80	[10]
	Fir (*Abies nordmanniana*) sawdust	28.1	86	[11]
	Chir pine (*Pinus roxburghii*) sawdust	5.8	72	[12]
	Eucalyptus (*Eucalyptus globulus*) sawdust	-	>80	[13]
Methylene Blue	White cedar sawdust	55.15	-	[14]
	Poplar waste biomass	21.9	98.50	[15]
	Pine sawdust (*Pinus strobus*)	10.3	99.94	[16]
	Cedar tree sawdust	142.36	-	[17]
Basic Violet 1	Chir pine (*Pinus roxburghii*) sawdust	11.3	96	[12]
Disperse Orange 30	Poplar sawdust	0.089	83.4	[18]
Eriochrome Black T	Sawdust unspecified	40.96	80	[19]
Allura Red AS	Sawdust unspecified	50.98	-	[20]
Safranine O	Sawdust unspecified	-	98	[21]

Compared to activated carbon and biochar, native lignocellulosic materials as biosorbents are mostly inferior, i.e., adsorption capacities of native materials are lower. Therefore, attempts have been made to improve the adsorption capacities of such materials by phys-

ical and/or chemical methods, including the production of biochar. However, from an economic perspective, the most affordable way to use lignocellulosic materials as biosorbents is to use them in their native form, if sufficiently high adsorption capacity and dye removal can be achieved.

CR is often used as a model dye in adsorption studies because of its complex chemical structure comprising two azo groups and multiple aromatic rings (Figure 1). Azo dyes are the most widely used class of synthetic organic dyes. CR was formerly commonly used in the textile industry, but many countries have banned it because of its toxicity—CR metabolizes into benzidine, a human mutagen and carcinogen [22]. However, it is still used as a stain in microbiology and diagnostic medicine (e.g., in the diagnosis of amyloidosis) [23], as well as a pH indicator.

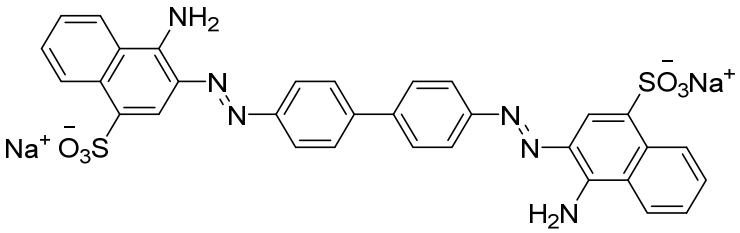

Figure 1. Chemical structure of Congo Red (CR).

This study aimed to screen the waste wood biomass of 10 different wood species prevalent in Croatia as biosorbents for CR removal from water and to single out the most efficient species. Furthermore, the effects of different factors, namely initial biosorbent concentration, contact time, initial CR concentration, and initial pH on the biosorption of CR on the waste biomass of the most efficient tree species from the screening experiment were investigated.

2. Materials and Methods

2.1. Biosorbents and Adsorbate

Croatian Forests Ltd. (branch Osijek, Croatia) and Croatian Forest Research Institute (Jastrebarsko, Croatia) kindly donated the waste wood biomass samples (shavings and sawdust remained after cutting the trees with the chainsaw) of 10 tree species. The following species were included: Common beech (*Fagus sylvatica* L.), pedunculate oak (*Quercus robur* L.), sessile oak (*Quercus petraea* (Matt.) Liebl.), common hornbeam (*Carpinus betulus* L.), narrow-leafed ash (*Fraxinus angustifolia* Vahl), Euroamerican poplar (*Populus euroamericana* Dode-Guinier), European silver fir (*Abies alba* Mill.), Norway spruce (*Picea abies* Karst.), European larch (*Larix decidua* Mill.), and Douglas fir (*Pseudotsuga menziesii* Mirb.). The selected tree species are prevalent in Croatian growing stock. Out of 10 selected species, four species were coniferous (European Silver Fir, Norway Spruce, European Larch, and Douglas Fir), while the remaining six species were deciduous trees.

The samples were oven-dried at 333.15 K for 48 h and milled using a laboratory knife mill (MF10 Basic, IKA Labortechnik, Staufen im Breisgau, Germany) equipped with 1 mm screen to obtain biosorbent particle size below 1 mm. Apart from drying and milling, no other treatments (physical or chemical) were applied.

2.2. Model Congo Red (CR) Solutions and Synthetic Wastewater Preparation

CR was purchased from Fisher Scientific. The stock solution of CR (1000 mg dm^{-3}) was prepared with demineralized water daily. Model CR solutions of different concentrations were prepared by diluting the stock solution to the desired concentration.

Synthetic wastewater was prepared by dissolving nutrients and minerals in demineralized water according to OECD guidelines 302B [24]. The composition of the synthetic wastewater was as follows: Peptone (160 mg dm^{-3}), meat extract (110 mg dm^{-3}), urea (30 mg dm^{-3}), K_2HPO_4 (28 mg dm^{-3}), NaCl (7 mg dm^{-3}), $CaCl_2 \cdot 2H_2O$ (4 mg dm^{-3}),

$MgSO_4 \cdot 7H_2O$ (2 mg dm^{-3}). For the preparation of synthetic wastewater with the addition of CR, the required amount of CR was added to the prepared synthetic wastewater up to a final dye mass concentration of γ_{CR} = 50 mg dm^{-3}. The pH of the synthetic wastewater with the addition of CR was pH = 7.56 (Seven Easy, Mettler Toledo, Greifensee, Switzerland).

2.3. Biosorbent Characterization

Characterization of all investigated biosorbents, namely elemental composition (CHN analysis), contents of ash, extractives, proteins and cellulose, point of zero charge (pH_{pzc}), and determination of surface functional groups (by Fourier transform infrared spectroscopy, FTIR) was given previously [15].

Further characterization of Euroamerican poplar (EP), as the most efficient biosorbent for CR removal in this study, included the investigation of EP surface morphology using field emission scanning electron microscope (FE-SEM, JSM-7000F, JOEL, Tokyo, Japan) and the comparison of the surface functional groups of EP before and after the biosorption of CR by recording the FTIR spectra from 4000 to 400 cm^{-1} (Cary 630, Agilent Technologies, Santa Clara, CA, USA).

2.4. Batch Biosorption Studies

The screening of biosorption properties of waste wood samples was carried out by the batch technique. A total of 25 cm^3 of CR model solution (γ_{CR} = 50 mg dm^{-3}) was added to 100 cm^3 Erlenmeyer flasks containing fixed amount (m = 0.25 g) of biosorbent. The experiments were carried out in a thermostatic shaker (SW22, JULABO GmbH, Seelbach, Germany) at the temperature of 298.15 K, the contact time of 360 min, and stirring speed of 150 rpm. pH was not adjusted, but it was measured at the beginning of the biosorption process using pH-meter (Seven Easy, Mettler Toledo, Greifensee, Switzerland). After 360 min the flasks were collected from the thermostatic shaker, filtered using Whatman filter paper No. 42, and centrifuged at 6000 rpm for 10 min (IKA mini G, IKA®-Werke GmbH & Co. KG, Staufen, Germany). The dye concentrations in supernatants were determined by ultraviolet-visible (UV/Vis) spectrophotometer at 498 nm (Specord 200, Analytic Jena, Jena, Germany). The percentage of CR removal and biosorption capacity q_e (mg g^{-1}) were calculated as follows:

$$\% \text{ CR removal} = \left[\frac{(\gamma_0 - \gamma_t)}{\gamma_0}\right] \cdot 100 \quad (1)$$

$$q_e = \frac{\gamma_0 - \gamma_e}{m} \cdot V \quad (2)$$

where γ_0, γ_t, and γ_e (mg dm^{-3}) are the initial CR concentration, CR concentration at a predetermined contact time, and CR concentration at equilibrium, respectively. V (dm^3) is the volume of the CR model solution, and m (g) is the mass of the biosorbent.

Biosorption Studies Using EP as Biosorbent

The effect of biosorbent concentration on the amount of CR adsorbed was investigated by varying the amount of biosorbent (from 0.025 g to 0.25 g) added to a definite volume (25 cm^3) of model CR solution, while keeping all other parameters constant (γ_{CR} = 50 mg dm^{-3}, t = 360 min, pH = 7, T = 298.15 K, v = 150 rpm). The effect of contact time was investigated at time intervals of 5, 15, 30, 60, 90, 120, 180, 240, 300, 360 min. To study the effect of the initial dye concentration on the amount of CR adsorbed, the initial CR concentrations were varied from 10 to 100 mg dm^{-3}, while all other parameters were kept constant ($\gamma_{biosorbent}$ = 8 g dm^{-3}, t = 360 min, pH = 7, T = 298.15 K, and v =150 rpm). The effect of pH was tested in the pH range from 4 to 9, while all other parameters were kept constant. The pH was adjusted using 0.1 mol dm^{-3} HCl and 0.1 mol dm^{-3} NaOH solutions.

The obtained experimental equilibrium data were analyzed using Langmuir and Freundlich isotherm models. To investigate the adsorption kinetics of CR onto EP, pseudo-first-order and pseudo-second-order kinetic models were used, as well as the intraparticle diffusion model. Duplicate experiments were conducted and were found reproducible.

3. Results and Discussion

3.1. Screening of Waste Biomass of Different Wood Species as Biosorbents for CR Removal

The results of waste wood biomass screening for CR removal are presented in Figure 2. EP proved to be the most efficient biosorbent for CR removal from water, achieving 71.8% CR removal and biosorption capacity of 3.3 mg g^{-1}. Second most efficient was common beach (51.1% CR removal and biosorption capacity of 2.2 mg g^{-1}), followed by European silver fir (42.3% CR removal and 1.8 mg g^{-1} biosorption capacity). Douglas fir was the least efficient with 13.1% CR removal and biosorption capacity of 0.5 mg g^{-1}. As reported previously [15], all the tested samples are characterized by high cellulose content and probably also by considerable hemicellulose and lignin contents [8]. The presence of many specific functional groups of these polymers usually favors the biosorptive removal of dyes. However, the difference in biosorption efficiency of the investigated tree species was significant. This could probably be attributed to the fact that despite the same preparation procedure, i.e., drying and milling, the degree of biomass fragmentation (particle size distribution, PSD) may be different for the tested materials since PSD is influenced by the material properties [25]. Even though not always investigated during the biosorption studies (including the present study), particle size can be an important factor affecting the biosorption process. Smaller biosorbent particles have a larger specific surface area, which means a larger number of biosorption sites are available for adsorbate binding and more efficient biosorption. However, when particles are very small, their separation from the water after biosorption could be challenging. Furthermore, out of the tested samples, poplars are characterized by the smallest specific density and (thus) the highest internal porosity [26,27], which could be the reason for the highest biosorption efficiency. The same 10 biosorbents were screened for cationic dye Methylene Blue (MB) removal under similar experimental conditions (different contact time, t = 120 min) and showed exceptional biosorptive capability with over 90% MB removal in all runs [15]. These results are consistent with the research by Nacu [28] who reported that adsorption capacity of sawdust for cationic dyes is much higher than that for anionic dyes (such as CR).

Based on the presented results, EP was singled out as the most efficient biosorbent for CR removal from water and was used in further experiments.

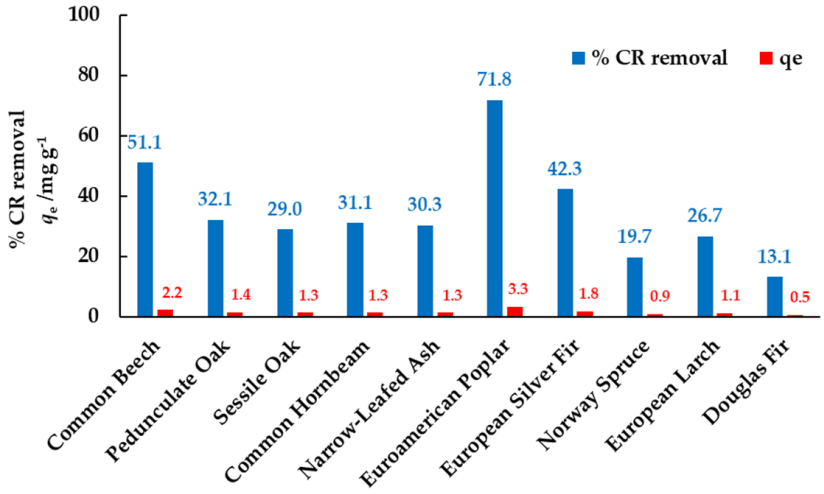

Figure 2. Screening of waste biomass of different wood species as biosorbents for CR removal from aqueous solutions (γ_{CR} = 50 mg dm^{-3}, $\gamma_{biosorbent}$ = 10 g dm^{-3}, t = 360 min, T = 298.15 K, v = 150 rpm).

3.2. Euroamerican Poplar (EP) Characterization

FE-SEM is a method often used to determine the morphological and structural characteristics of the biosorbent surface. FE-SEM micrographs taken at different magnifications are shown in Figure 3. The surface of the EP is heterogeneous, rough, and uneven. Nacu [28] reported that the texture properties of sawdust and bark of different tree species are characterized by the presence of micro-, meso-, and macro- pores, with the predominant mesoporous structure of waste wood biomass. The described morphology favorably affects the binding of adsorbate molecules [29].

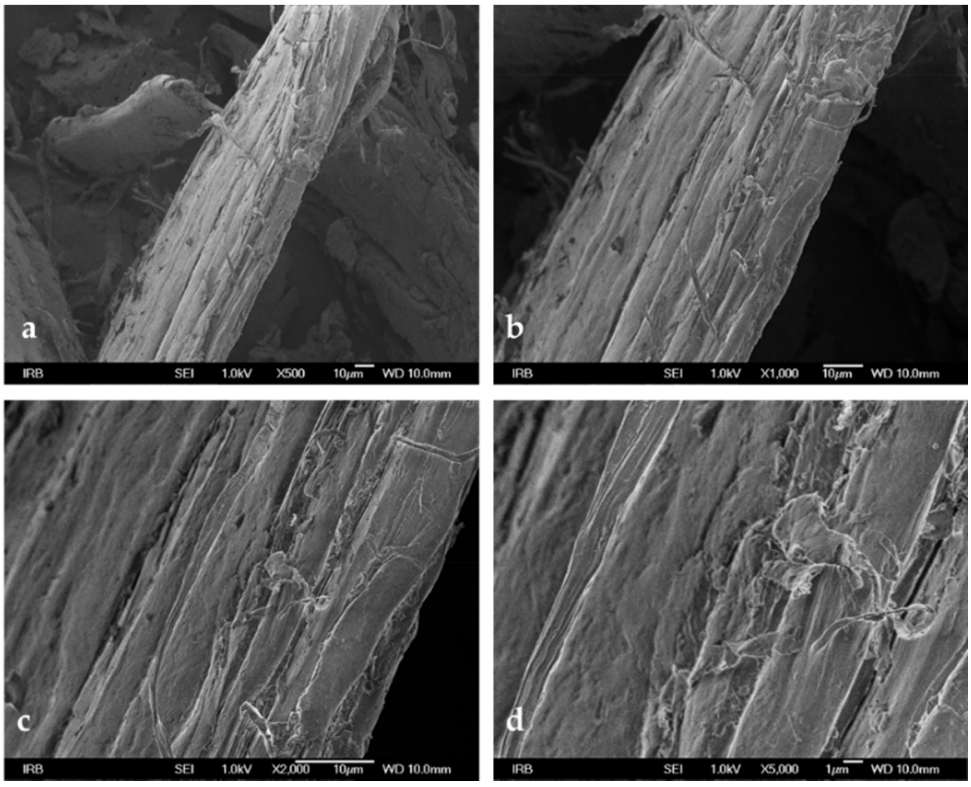

Figure 3. Field emission scanning electron microscopy (FE-SEM) micrographs of Euroamerican poplar (EP) at different magnifications: (**a**) 500, (**b**) 1000, (**c**) 2000, (**d**) 5000.

Qualitative analysis of specific functional groups on the biosorbent surface, which affect the efficiency of the biosorption process, is commonly performed using the FTIR method. The FTIR spectra of EP before and after dye biosorption are shown in Figure 4.

The very wide band dominates both spectra at 3339.7 cm^{-1} (3324.8 for CR loaded EP), which can be attributed to hydroxyl groups (-OH), i.e., vibrations of OH bond stretching, probably connected to inter- and intramolecular formation of hydrogen bonds within cellulose and lignin. The second most prominent band is the 1028.7 cm^{-1} intense band, that could be assigned to the polysaccharides, i.e., C-O, C=C, and C-C-O stretching in lignin, cellulose, and hemicellulose. The band with a maximum at 2914.8 cm^{-1} could be associated with the stretching of aliphatic groups (-CH). The 1729.5 (1736.9 for CR loaded EP) band can be assigned to C=O stretching [30]. The presence of branched-chain aromatic radicals is indicated by bands from 1423.8 to 1505.8 cm^{-1} [31]. The slight shifting of the peaks (frequency and intensity change) in the FTIR spectrum of CR loaded EP compared to that of EP could be assigned to the biosorption of CR on the surface of biosorbent. As reported previously [15], EP used in this study is comprised of a large portion of cellulose (40.53%). The presence of cellulose, hemicellulose, and lignin, with a substantial number of functional groups present at the biosorbent surface, favorably affects the removal of dyes. In general, the adsorption takes place by hydrogen bonding, complexation, and

ion exchange [32]. High contents of cellulose, hemicellulose, and lignin, with a large number of hydroxyl, carbonyl, and carboxyl functional groups, allow retention of dyes and even metals from aqueous solutions. In most cases this occurs through the ion exchange mechanism in which such materials behave as shifters of natural ions [33,34].

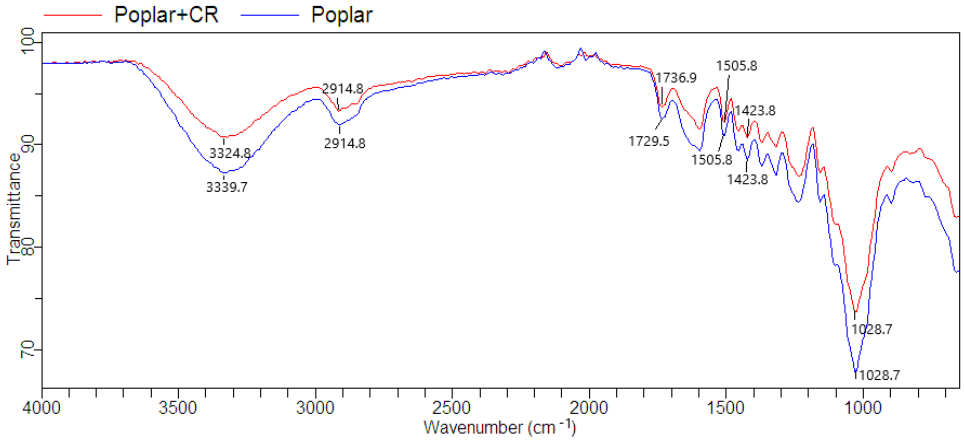

Figure 4. The Fourier transform infrared spectroscopy (FTIR) spectral characteristics of EP before and after CR biosorption.

3.3. Biosorption Studies Using EP as Biosorbent

3.3.1. The Effect of Biosorbent Concentration

The adsorbent concentration is an important parameter that affects the adsorption process and defines the adsorption capacity of the adsorbent at the selected initial adsorbate concentration [35]. Since the number of sorption sites at the adsorbent surface increases by increasing the adsorbent concentration, generally, the percentage of dye removal will also increase [36]. In order to determine the optimal concentration of biosorbent to be used in further experiments, different biosorbent concentrations (1–10 g dm^{-3}) were tested, and the obtained results are shown in Figure 5.

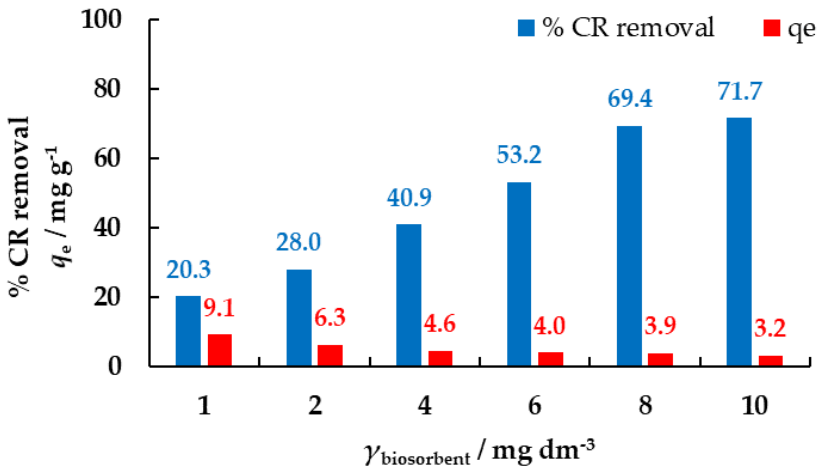

Figure 5. The effect of biosorbent concentration on the biosorption of CR to EP (γ_{CR} = 50 mg dm^{-3}, t = 360 min, pH = 7, T = 298.15 K, v = 150 rpm).

Increase of the biosorbent concentration led to an increase of the CR removal percentage, but also a simultaneous decrease of biosorption capacity. The results show that the percentage of CR removal increased from 20.3% to 71.7% with an increase of biosorbent concentration from 1 to 10 mg dm^{-3}. However, when biosorbent concentration increased from 6 to 8 g dm^{-3} the incremental CR percentage removal became small. This is in accordance with other authors who reported the increase in dye removal percentage with the increasing

biosorbent concentration up to a concentration when removal percentage reaches a constant value [13,15,30]. The biosorption capacity decreased from 9.1 to 3.2 mg g^{-1} with the increasing biosorbent concentration. The decrease in biosorption capacity can probably be attributed to the increase of the area available for binding of the same amount of adsorbate, whereby a smaller amount of adsorbate per unit mass of biosorbent is adsorbed.

Increase of the dye removal percentage with increasing the biosorbent concentration is consistent with the results of other studies dealing with biosorption of dyes, such as CR biosorption on fir sawdust biomass [11], Eucalyptus wood sawdust [13], *E. crassipes* root [37], and cattail root [38], as well as MB biosorption on EP waste biomass [15] and meranti sawdust [30].

Taking into consideration both CR removal percentage and biosorption capacity, biosorbent concentration of 8 mg dm^{-3} was selected for further experiments.

3.3.2. The Effect of Contact Time

Adsorption depends on the contact time between the adsorbent and the adsorbate. Fast adsorption of the adsorbate from the liquid phase and quick establishment of equilibrium are some of the good adsorbent characteristics. Determining the optimal adsorption contact time is essential for both process optimization and the application of an adsorbent in real wastewater treatment systems. From the results shown in Figure 6, it can be seen that the removal of CR by EP is characterized by rapid removal during the initial stages (the first 60 min) of biosorption. At the initial stages, the surface available for dye biosorption is large, and the process mainly occurs at the biosorbent surface [38]. After the initial rapid removal of the dye, in the later stages of the experiment, the removal rate decreases until equilibrium is reached (within 180 min). At this stage, the dye is transported from the sites at biosorbent surface to the internal sites of the biosorbent, so the dye removal gets slower [37,38]. To ensure the equilibrium is reached, the contact time of 360 min was applied in further experiments.

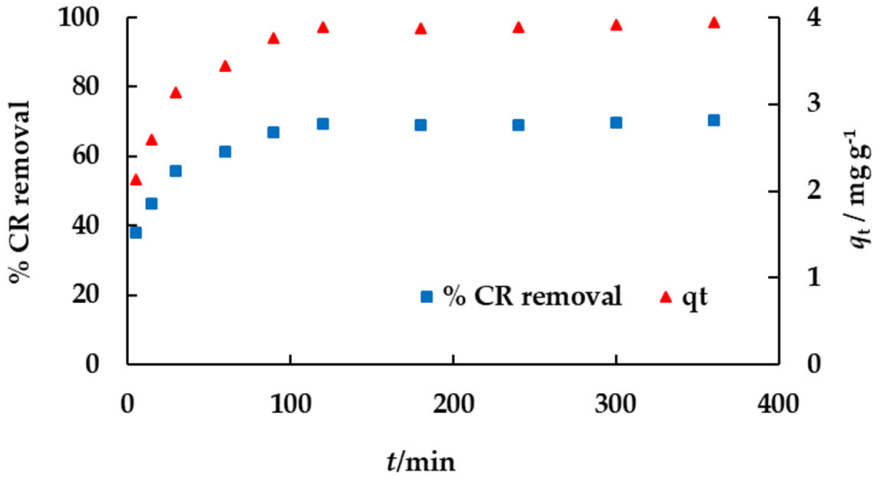

Figure 6. The effect of contact time on the biosorption of CR to EP (γ_{CR} = 50 mg dm^{-3}, $\gamma_{biosorbent}$ = 8 mg dm^{-3}, pH = 7, T = 298.15 K, v = 150 rpm).

3.3.3. The Effect of Initial CR Concentration

The effect of the initial CR concentration on the percentage CR removal and biosorption capacity is presented in Figure 7. By increasing the initial dye concentration from 10 to 100 mg dm^{-3}, the percentage of dye removal decreased from 85.6% to 49.6%, while the biosorption capacity increased from 1.1 to 6.2 mg g^{-1}. At higher concentrations of adsorbate, the number of occupied biosorption sites is higher, so the biosorption capacity increases. At the same time, the efficiency of the adsorbate removal process (expressed as percentage dye removal) in general will decrease, probably as a result of the saturation of surface biosorption sites [36]. The results indicate that the removal of CR by biosorption on

EP is a dye concentration-dependent process, which is consistent with the results of other authors who used other lignocellulosic biosorbents for CR removal such as the Eucalyptus wood sawdust [13], chir pine sawdust [12], the roots of the plant *E. crassipes* [37], and the cattail root [38]. The resistance to transfer dye molecules between the liquid and solid phase is more easily overcome at higher initial dye concentrations, because of the higher driving force (higher concentration gradient) provided. Consequently, the amount of dye adsorbed per unit mass of biosorbent, as well as the rate of biosorption at equilibrium increase [13,36,39].

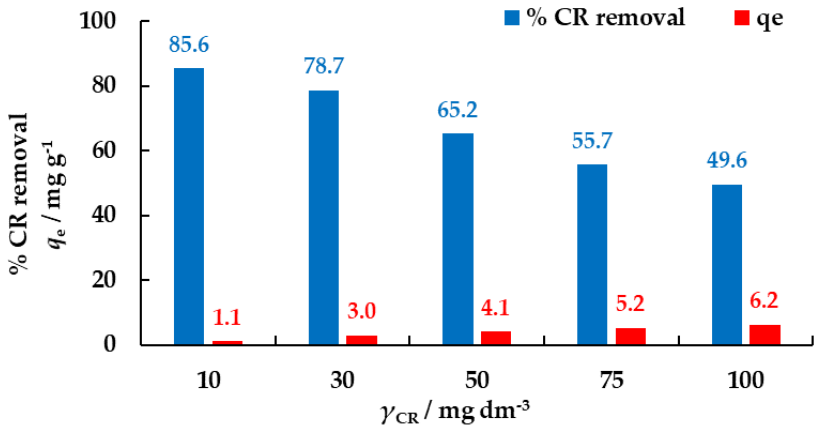

Figure 7. The effect of initial CR concentration on biosorption to EP ($\gamma_{biosorbent}$ = 8 mg dm^{-3}, t = 360 min, pH = 7, T = 298.15 K, v = 150 rpm).

3.3.4. The Effect of pH

Solution pH is the factor significantly affecting the efficiency of adsorbent during the wastewater treatment. A change in the pH of the system in which the adsorption process takes place can lead to the change in the active site of the biosorbent, as well as to a change in the charge (degree of ionization) of the dye itself [36,40]. The effect of the pH on the biosorption capacity of EP and the percentage of CR removal was tested over the pH range from 4 to 9 and is shown in Figure 8.

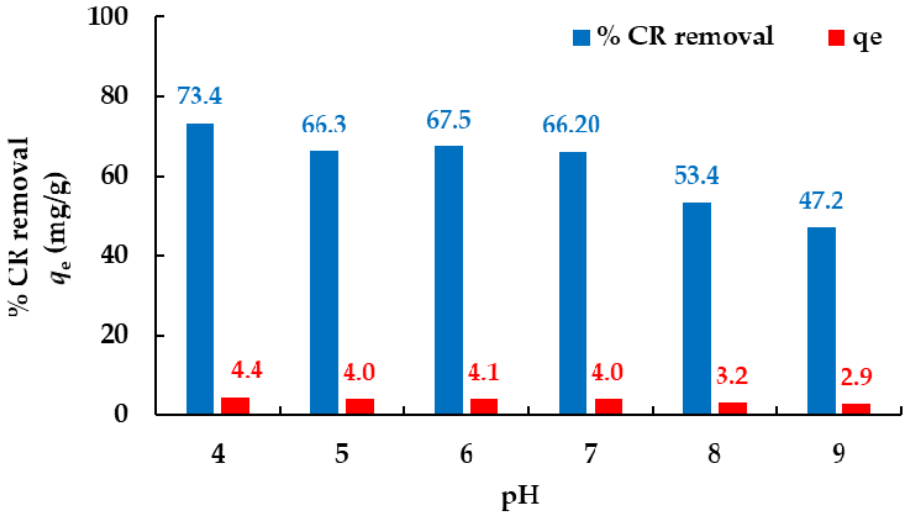

Figure 8. The effect of pH on biosorption of CR to EP (γ_{CR} = 50 mg dm^{-3}, $\gamma_{biosorbent}$ = 8 mg dm^{-3}, t = 360 min, T = 298.15 K, v = 150 rpm).

The highest percentage of CR removal (73.4%) and the highest biosorption capacity (4.4 mg g^{-1}) were achieved at pH = 4. In the pH range from 5 to 7 both the percentage CR removal and biosorption capacity were almost constant (66.20–67.5% and 4.0–4.1 mg g^{-1},

respectively) and only slightly lower than the values achieved at pH = 4. On the other hand, at basic pH value (pH = 8–9) a considerable drop of percentage CR removal and biosorption capacity was noticed. When considering the effect of pH on adsorption process, it is valuable to know the pH value that corresponds to a pH at which the adsorbent surface charge density is equal to zero (i.e., point of zero charge, pH_{pzc}). pH_{pzc} of EP was reported to be pH_{pzc} = 7.1 [15]. Knowing the pH_{pzc} of the adsorbent is important to understand better the electrostatic interactions between the adsorbent surface and the adsorbate at a given pH. Theoretically, at pH < pH_{pzc} the surface of the adsorbent is positively charged, which is the condition conducive to the adsorption of anionic dyes, such as CR. On the other hand, at pH > pH_{pzc} the surface of the adsorbent is negatively charged, which favors the adsorption of cationic dyes [41]. More efficient biosorption of CR at lower pH values was confirmed by Ribeiro et al. [10] who used wood sawdust powder from Eucalyptus *Corymbia citriodora* as biosorbent, by Khan et al. [12] who used chir pine sawdust, as well as by Chanzu et al. [42] who used brewers' spent grains as biosorbent. At lower pH values cationic dyes compete for adsorption sites with H^+ ions, while anionic dyes compete with OH^- ions at higher pH values, which in both cases negatively affects the adsorption efficiency [42]. The results obtained in this study differ slightly from the results of [38] who reported the highest CR removal percentage using cattail root at pH = 5, but constant removal percentage over the pH range from 5.5 to 10. Li et al. [43] who used cassava waste and Jain and Sikarwar [44] who used activated de-oiled mustard as biosorbents for CR removal reported that pH did not significantly affect the biosorption capacity of the applied lignocellulosic materials. Furthermore, Mane and Vijay Babu [13] reported that CR solution is stable at pH =7, but gets unstable if solution pH is lower or higher. They also reported the maximum percentage of CR removal at pH = 7. Over the pH range from 4 to 10, more than 80% of CR was removed. The percentage CR removal increased (from 80% to 85%) with the increase in pH from 4 to 7, while it slightly decreased over the pH range from 7 to 10. At pH > 10, they reported a significant decrease in percentage CR removal.

3.3.5. Biosorption of CR to EP from Synthetic Wastewater

Model dye solutions are commonly used when investigating the applicability of adsorbents for dye removal, especially when dealing with unconventional (low-cost) adsorbents, i.e., biosorbents. However, the composition of real wastewater is much more complex, with many (dissolved and undissolved) pollutants and other substances that can affect the bio-sorption process. To further explore the possible use of EP as biosorbent, biosorption of CR to EP from synthetic wastewater with the addition of CR was investigated, and the results are presented in Figure 9.

The percentage of CR removal from synthetic wastewater after 360 min was 18.6% higher than from model CR solution. During the first 60 min, characterized by rapid CR removal, the percentage of CR removal from synthetic wastewater was even higher (28.2%). This can probably be explained by the fact that the ionic strength of wastewater is higher than that of model dye solutions. Hu et al. [38] reported the increase of CR removal by cattail root with the increase of ionic strength of NaCl from 0 to 0.1 mol dm^{-3}. They stated that the ionic strength increase would result in the increase of the positive charge of adsorbent surface and the electrostatic interaction between the dye and adsorbent will increase.

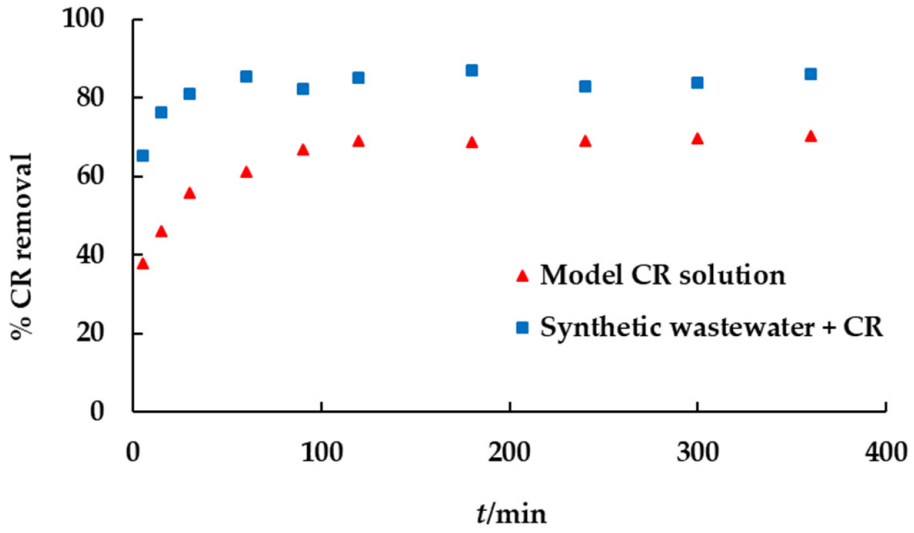

Figure 9. Biosorption of CR to EP from model CR solution and synthetic wastewater with the addition of CR (γ_{CR} = 50 mg dm^{-3}, $\gamma_{biosorbent}$ = 8 mg dm^{-3}, t =360 min, T = 298.15 K, v = 150 rpm).

3.3.6. Adsorption Isotherms

To describe how adsorbate molecules are distributed between the liquid and solid phases at equilibrium and to provide insight into the maximum adsorption capacity of an adsorbent for adsorbate, adsorption isotherms are used [45]. Langmuir and Freundlich adsorption isotherms are the most commonly used mathematical models for this purpose. Langmuir and Freundlich isotherm plots for CR biosorption on EP are shown in Figure 10, while the obtained isotherm parameters are given in Table 2.

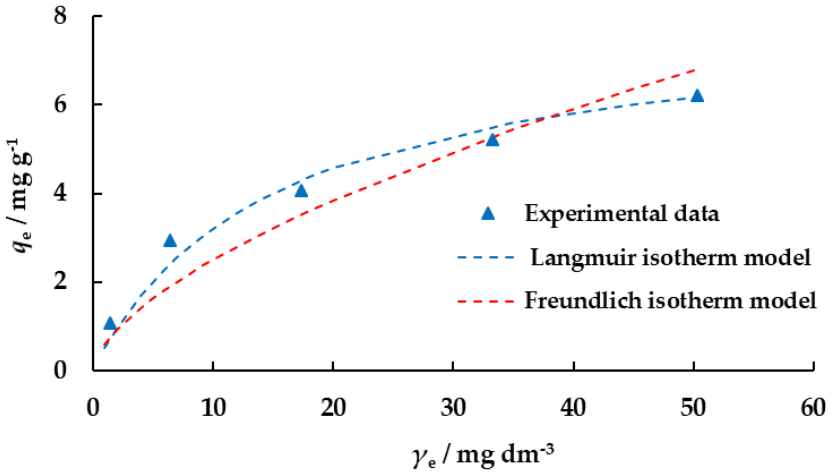

Figure 10. Langmuir and Freundlich isotherms of CR biosorption on EP ($\gamma_{biosorbent}$ = 8 mg dm^{-3}, t = 360 min, pH = 7, T = 298.15 K, v = 150 rpm).

Langmuir adsorption isotherm model assumes the adsorbent molecules are adsorbed in only one layer (monolayer), all available adsorption sites are homogenous, and their number is fixed, and the adsorption process is reversible [46]. The Langmuir isotherm equation [47] is expressed as follows:

$$q_e = \frac{q_m \cdot K_L \cdot \gamma_e}{1 + K_L \cdot \gamma_e} \quad (3)$$

where γ_e (mg dm^{-3}) is the CR concentration at equilibrium, q_e (mg g^{-1}) is the amount of CR adsorbed per unit mass of adsorbent, q_m (mg g^{-1}) is the maximum amount of

CR adsorbed (to form a surface monolayer, i.e., monolayer adsorption capacity), and K_L ($dm^3\ mg^{-1}$) is the Langmuir constant. The dimensionless constant R_L (equilibrium parameter) indicates the type of isotherm to be favorable ($0 < R_L < 1$), unfavorable ($R_L > 1$), linear ($R_L = 1$), or irreversible ($R_L = 0$). It can be calculated as follows [46]:

$$R_L = \frac{1}{1 + K_L \cdot \gamma_o} \quad (4)$$

where γ_0 ($mg\ dm^{-3}$) is the highest initial concentration of dye. The R_L value presented in Table 2 is 0.130, which indicates that biosorption of CR on EP under the applied experimental conditions was a favorable process.

Table 2. Isotherm parameters for the removal of CR by EP at 298.15 K.

Isotherm Model	CR
$q_{m\ exp.}$/mg g^{-1}	6.21
Langmuir	
$q_{m\ cal.}$/mg g^{-1}	8.00
K_L/dm^3 mg^{-1}	0.067
R_L	0.130
se	0.441
Freundlich	
K_F/(mg/g $(dm^3/mg)^{1/n}$)	0.60
n	1.61
se	0.794

The Freundlich adsorption isotherm is used to describe adsorption in a multilayer (on heterogeneous surfaces) where there are interactions between adsorbate molecules. The Freundlich isotherm can be expressed by the following equation [48]:

$$q_e = K_f \gamma_e{}^{\frac{1}{n}} \quad (5)$$

where q_e ($mg\ g^{-1}$) is the adsorbed amount of dye at equilibrium, γ_e ($mg\ dm^{-3}$) is the concentration of dye in solution at equilibrium, K_F is the constant indicating adsorption capacity of adsorbent, and n indicates the intensity of adsorption. When $n = 1$ adsorption is linear, $n < 1$ adsorption is a chemical process, and $n > 1$ indicates a physical process that is favorable [49]. The value of the constant n in this study was 1.61, which indicates a physical process that is favorable.

By analyzing these values for both models presented in Table 2, as well as the Langmuir and Freundlich isotherm plots for CR biosorption on EP given in Figure 10, it seems that the Langmuir model better describes the experimentally obtained data.

3.3.7. Adsorption Kinetics

Research on the kinetics of the adsorption process is important because it provides information on the possible adsorption mechanisms and a theoretical basis for the development and application of adsorbents on an industrial scale [50]. Thus, knowing the batch adsorption kinetics is vital for the industrial adsorption columns design [13]. The results of the experimental data modelling using two selected kinetic models—the pseudo-first-order model and the pseudo-second-order model—are given in Table 3.

Table 3. Parameters of the pseudo-first-order and pseudo-second-order kinetic models for the removal of CR by EP (γ_{CR} = 50 mg dm^{-3}, $\gamma_{biosorbent}$ = 8 mg dm^{-3}, t =360 min, pH = 7, T = 298.15 K, v = 150 rpm).

	Pseudo-First Order				Pseudo-Second Order		
Parameter							
γ_0/mg dm^{-3}	$q_{e\,exp}$/mg g^{-1}	k_1/min^{-1}	$q_{e\,cal}$/mg g^{-1}	R^2	k_2/g mg^{-1} min^{-1}	$q_{e\,cal.}$/mg g^{-1}	R^2
50	3.95	0.061	1.063	0.837	0.035	4.023	0.9998

Lagergren pseudo-first-order model [51] that can be applied for the liquid/solid system adsorption and assumes that the adsorption rate is proportional to the number of unoccupied sites (by solutes) [52] is represented by the following equation:

$$\ln(q_e - q_t) = lnq_e - k_1 t \quad (6)$$

where q_e is the amount of dye adsorbed at equilibrium, q_t (mg g^{-1}) is the amount of dye adsorbed at time t (min), and k_1 (min^{-1}) is the pseudo-first-order rate constant.

According to Ho and McKay [53], pseudo-second-order model is expressed as:

$$\frac{1}{q_t} - \frac{1}{q_e} = \frac{1}{k_2 \cdot q_e^2 \cdot t} \quad (7)$$

where k_2 (g mg^{-1} min^{-1}) is the pseudo-second-order rate constant. The pseudo-second-order model assumes that both adsorption and ion exchange take place on the adsorbent surface, with the limiting factor of the adsorption rate being the chemical binding to active sites on the adsorbent surface [54].

The results presented in Table 3 suggest that the biosorption of CR on EP under the applied experimental conditions is more appropriately approximated by the pseudo-second-order model. The goodness of fit was based on the values of the linear regression correlation coefficient R^2 and the agreement of calculated $q_{e\,cal}$ values and the experimental $q_{e\,exp}$ values. Apart from R^2 being closer to unity for the pseudo-second-order model, the values of $q_{e\,cal}$ and $q_{e\,exp}$ for the pseudo-second-order model are in a better agreement than for the pseudo-first-order model. This is in line with other studies reporting the pseudo-second-order kinetic model as the best-fit model for the prediction of the batch adsorption kinetics of CR on different biosorbents [13,37,38,55].

Adsorption is a multistage process, in which the adsorbate is transferred from the solution to the solid phase into the interior of the adsorbent where it is retained [56]. To explain the diffusion mechanism, the experimental data were analyzed by the intraparticle diffusion model, and the graphical dependence q_t with $t^{0.5}$ is shown in Figure 11, while the model parameters are given in Table 4.

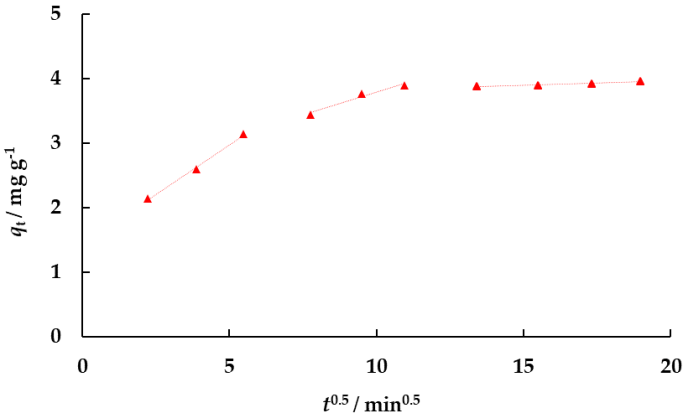

Figure 11. Weber and Morris intraparticle diffusion plot for CR removal using EP (γ_{CR} = 50 mg dm^{-3}, $\gamma_{biosorbent}$ = 8 mg dm^{-3}, t =360 min, pH = 7, T = 298.15 K, v = 150 rpm).

Table 4. Parameters of the Weber and Morris intraparticle diffusion model for the removal of CR by EP (γ_{CR} = 50 mg dm^{-3}, $\gamma_{biosorbent}$ = 8 mg dm^{-3}, t =360 min, pH = 7, T = 298.15 K, v = 150 rpm, * mg g^{-1} min$^{-0.5}$).

Intraparticle Diffusion Model Parameter									
γ_0/ mg dm^{-3}	k_{i1} *	C_1	$R_1{}^2$	k_{i2} *	C_2	$R_2{}^2$	$k_{i\,3}$ *	C_3	$R_3{}^2$
50	0.3089	14.329	0.9974	0.1419	23.678	0.9651	0.0143	36.758	0.9636

The intraparticle diffusion model was proposed by Weber and Morris [57]. The effect of intraparticle diffusion resistance on adsorption process can be evaluated using the equation:

$$q_t = k_i \times t^{1/2} + C \quad (8)$$

where k_i (mg g^{-1} min$^{-0.5}$) is the intraparticle diffusion rate constant, and C is constant that describes the thickness of the boundary layer. Since C is proportional to the thickness, a larger value indicates the more profound boundary layer effect, but also indicates higher adsorption capacity [55]. When the plot of q versus $t^{1/2}$ passes through the origin (Figure 11, intraparticle diffusion is the only rate-limiting step. On the other hand, if C $\neq$ 0, boundary layer diffusion is controlling the adsorption to a certain level. Three linear regions are visible in Figure 11. This multilinearity suggests that intraparticle diffusion is not the only step limiting the rate of biosorption of CR to EP. The first linear region, which is the steepest, can probably be attributed to biosorption on the outer surface of the biosorbent (i.e., diffusion in the film). The other two linear regions are less steep and are attributed to the phase in which adsorption is slower and the equilibrium phase when the effect of intraparticle diffusion is much smaller or completely stopped, due to the low concentration of adsorbate in the solution.

4. Conclusions

This study investigated the applicability of waste wood biomass of ten tree species for the biosorptive removal of Congo Red (CR) from water. Euroamerican poplar (EP) was singled out as the most efficient biosorbent for CR removal, achieving 71.8% CR removal and biosorption capacity of 3.3 mg g^{-1}, and was used for further batch biosorption experiments. The CR biosorption on EP was found to be strongly dependent on biosorbent concentration, contact time, initial CR concentration, and pH. The equilibrium was achieved within 180 min. The process could be interpreted in terms of the Langmuir adsorption isotherm model. The pseudo-second-order kinetic model well described the kinetic data of the biosorption process. Intraparticle diffusion was not the only process controlling the biosorption of CR on EP. The results presented in this study suggest that the EP has the potential to be used as a low-cost biosorbent for CR removal from dye-loaded wastewater. With the aim of possible utilization of waste wood biomass of other tree species included in the screening experiments, future research should include more detailed characterization of these materials including the pore size and volume analysis, the surface area analysis, and the study of the effect of biosorbent specific density, porosity, and particle size on the biosorption efficiency. Furthermore, future research directions should focus on waste wood modifications to improve the biosorption capacity, as well as on column studies that are more industrially feasible for real wastewater treatment systems.

Author Contributions: Conceptualization, methodology, M.S. and N.V.; formal analysis, M.S. and N.V.; investigation, M.S., A.G., and I.K.; resources, N.V., T.J., and M.H.-S.; writing—original draft preparation, M.S. and I.K. writing—review and editing, N.V., M.H.-S., and T.J.; visualization, M.S. and N.V.; funding acquisition, N.V., M.S., and M.H.-S. All authors have read and agreed to the published version of the manuscript.

Funding: This research received no external funding.

Institutional Review Board Statement: Not applicable.

Informed Consent Statement: Not applicable.

Data Availability Statement: Not applicable.

Acknowledgments: Authors wish to thank Mirela Kopjar, Faculty of Food Technology Osijek, University of Osijek, for FTIR spectra recordings using the equipment funded by the project HRZZ-UIP-2013-11-6949.

Conflicts of Interest: The authors declare no conflict of interest.

References

1. Uasuf, A.; Becker, G. Wood pellets production costs and energy consumption under different framework conditions in Northeast Argentina. *Biomass Bioenerg.* **2011**, *35*, 1357–1366. [CrossRef]
2. Ejder-Korucu, M.; Gürses, A.; Doğar, Ç.; Sharma, S.K.; Açıkyıldız, M. Removal of Organic Dyes from Industrial Effluents: An Overview of Physical and Biotechnological Applications. In *Green Chemistry for Dyes Removal from Wastewater*, 1st ed.; Sharma, S.K., Ed.; Scrivener Publishing: Beverly, MA, USA, 2015; pp. 1–22.
3. Mathur, N.; Bhatnagar, P.; Bakre, P. Assessing mutagenicity of textile dyes from Pali (Rajasthan) using ames bioassay. *Appl. Ecol. Environ. Res.* **2006**, *4*, 111–118. [CrossRef]
4. Puvaneswari, N.; Muthukrishnan, J.; Gunasekaran, P. Toxicity assessment and microbial degradation of azo dyes. *Indian J. Exp. Biol.* **2006**, *44*, 618–626. [PubMed]
5. Yesilada, O.; Asma, D.; Cing, S. Decolorization of textile dyes by fungal pellets. *Process Biochem.* **2003**, *38*, 933–938. [CrossRef]
6. Crini, G. Non-conventional low-cost adsorbents for dye removal: A review. *Bioresor. Technol.* **2006**, *97*, 1061–1085. [CrossRef] [PubMed]
7. Michalak, I.; Chojnacka, K.; Witek-Krowiak, A. State of the art for the biosorption process—A review. *Appl. Biochem. Biotechnol.* **2013**, *170*, 1389–1416. [CrossRef] [PubMed]
8. Sjostrom, E. *Wood Chemistry. Fundamentals and Applications*, 2nd ed.; Academic press: San Diego, CA, USA, 1993; p. 292.
9. Litefti, K.; Freire, M.S.; Stitou, M.; González-Álvarez, J. Adsorption of an anionic dye (Congo red) from aqueous solutions by pine bark. *Sci. Rep.* **2019**, *9*, 1–11. [CrossRef]
10. Ribeiro, A.V.F.N.; da Silva, A.R.; Pereira, M.G.; Licinio, M.V.V.J.; Ribeiro, J.N. Wood sawdust powder from *Corimbya citriodora* to congo red toxic dye adsorption. *Indian J. Appl. Res.* **2018**, *8*, 29–31. [CrossRef]
11. Burcă, S.; Indolean, C.; Măicăneanu, A. Isotherms study of congo red biosorption equilibrium using FIR (*Abies Nordmanniana*) sawdust biomass. *Rev. Roum. Chim.* **2017**, *62*, 381–389.
12. Khan, T.A.; Sharma, S.; Khan, E.A.; Mukhlif, A.A. Removal of congo red and basic violet 1 by chir pine (*Pinus roxburghii*) sawdust, a saw mill waste: Batch and column studies. *Toxicol. Environ. Chem.* **2014**, *96*, 555–568. [CrossRef]
13. Mane, V.S.; Vijay Babu, P.V. Kinetic and equilibrium studies on the removal of Congo red from aqueous solution using Eucalyptus wood (*Eucalyptus globulus*) sawdust. *J. Taiwan Inst. Chem. Eng.* **2013**, *44*, 81–88. [CrossRef]
14. Gardazi, S.M.H.; Shah, J.A.; Ashfag, T.; Sherazi, T.A.; Ali, M.A.; Pervez, A.; Rashid, N. Equilibrium, kinetics and thermodynamic study of the adsorptive removal of methylene blue from industrial wastewater by white cedar sawdust. *Environ. Prot. Eng.* **2019**, *45*, 5–22. [CrossRef]
15. Velić, N.; Stjepanović, M.; Begović, L.; Habuda-Stanić, M.; Velić, D.; Jakovljević, T. Valorisation of waste wood biomass as biosorbent for the removal of synthetic dye methylene blue from aqueous solutions. *South-East Eur. For.* **2018**, *9*, 115–122. [CrossRef]
16. Salazar-Rabago, J.J.; Leyva-Ramos, R.; Rivera-Utrilla, J.; Ocampo-Perez, R.; Cerino-Cordova, F.J. Biosorption mechanism of Methylene Blue from aqueous solution onto White Pine (*Pinus durangensis*) sawdust: Effect of operating conditions. *Sustain. Environ. Res.* **2017**, *27*, 32–40. [CrossRef]
17. Hamdaoui, O. Batch study of liquid-phase adsorption of methylene blue using cedar sawdust and crushed brick. *J. Hazard. Mater.* **2006**, *135*, 264–273. [CrossRef]
18. Tezcan Un, U.; Ates, F. Low-cost adsorbent prepared from poplar sawdust for removal of disperse orange 30 dye from aqueous solutions. *Int. J. Environ. Sci. Technol.* **2019**, *16*, 899–908. [CrossRef]
19. Akhouairi, S.; Ouachtak, H.; Addi, A.A.; Jada, A.; Douch, J. Natural Sawdust as Adsorbent for the Eriochrome Black T Dye Removal from Aqueous Solution. *Water Air Soil Poll.* **2019**, *230*, 181. [CrossRef]
20. Saha, T.K.; Bishwas, R.K.; Karmaker, S.; Islam, Z. Adsorption Characteristics of Allura Red AC onto Sawdust and Hexadecylpyridinium Bromide-Treated Sawdust in Aqueous Solution. *ACS Omega* **2020**, *5*, 13358–13374. [CrossRef]
21. Saroha, A.; Ghosh, A. Biosorption of Safranine O Dye by SawDust. In *Advances in Water Pollution Monitoring and Control*; Springer Transactions in Civil and Environmental Engineering; Siddiqui, N., Tauseef, S., Dobhal, R., Eds.; Springer: Singapore, 2020. [CrossRef]
22. Asses, N.; Ayed, L.; Hkiri, N.; Hamdi, M. Congo Red Decolorization and Detoxification by *Aspergillus niger*: Removal Mechanisms and Dye Degradation Pathway. *BioMed Res. Int.* **2018**, 3049686. [CrossRef]

23. Clement, C.G.; Truong, L.D. An evaluation of Congo red fluorescence for the diagnosis of amyloidosis. *Hum. Pathol.* **2014**, *45*, 1766–1772. [CrossRef]
24. OECD. *Guideline for Testing of Chemicals*; Test Guidline 302 B; OECD: Paris, France, 1992.
25. Jewiarz, M.; Wróbel, M.; Mudryk, K.; Szufa, S. Impact of the Drying Temperature and Grinding Technique on Biomass Grindability. *Energies* **2020**, *13*, 3392. [CrossRef]
26. Niemczyk, M.; Kaliszewski, A.; Jewiarz, M.; Wróbel, M.; Mudryk, K. Productivity and biomass characteristics of selected poplar (*Populus* spp.) cultivars under the climatic conditions of northern Poland. *Biomass Bioenergy* **2018**, *111*, 46–51. [CrossRef]
27. Karbowniczak, A.; Hamerska, J.; Wróbel, M.; Jewiarz, M.; Nęcka, K. Evaluation of Selected Species of Woody Plants in Terms of Suitability for Energy Production. In *Renewable Energy Sources: Engineering, Technology, Innovation*; Springer Proceedings in Energy; Mudryk, K., Werle, S., Eds.; Springer: Cham, Switzerland, 2018; pp. 735–742. [CrossRef]
28. Nacu, G. Studies on the Use of Cellulosic Waste to Reduce Environmental Pollution. Ph.D. Thesis, Technical University "Gheorghe Asachi" of Iaşi, Iaşi, Romania, 2015.
29. Da Silva, B.C.; Zanutto, A.; Pietrobelli, M.T.A.J. Biosorption of reactive yellow dye by malt bagasse. *Adsorpt. Sci. Technol.* **2019**, *37*, 236–259. [CrossRef]
30. Ahmad, A.; Rafatullah, M.; Sulaiman, O.; Ibrahim, M.H.; Hashim, R. Scavenging behaviour of meranti sawdust in the removal of methylene blue from aqueous solution. *J. Hazard. Mater.* **2009**, *170*, 357–365. [CrossRef]
31. Pistorius, A.M.A.; DeGrip, W.J.; Egorova-Zachernyuk, T.A. Monitoring of Biomass Composition from Microbiological Sources by Means of FT-IR Spectroscopy. *Biotechnol. Bioeng.* **2009**, *103*, 123–129. [CrossRef]
32. Adegoke, K.A.; Bello, O.S. Dye sequestration using agricultural wastes as adsorbents. *Water Resour. Ind.* **2015**, *12*, 8–24. [CrossRef]
33. Shin, E.W.; Karthikeyan, K.G.; Tshabalala, M.A. Adsorption mechanism of cadmium on juniper bark and wood. *Bioresour. Technol.* **2007**, *98*, 588–594. [CrossRef]
34. Suteu, D.; Rusu, G.; Zaharia, C. Removal of reactive dye Orange 16 from aqueous solution by sorption onto sawdust. *Chem. Bull. Politeh. Univ.* **2011**, *56*, 24–28.
35. Bulut, Y.; Aydin, H. A kinetics and thermodynamics study of methylene blue adsorption on wheat shells. *Desalination* **2006**, *194*, 259–267. [CrossRef]
36. Yagub, M.T.; Sen, T.K.; Afroze, S.; Ang, H.M. Dye and its removal from aqueous solution by adsorption: A review. *Adv. Colloid Interface Sci.* **2014**, *209*, 172–184. [CrossRef]
37. Wanyonyi, W.; Onyari, J.; Shiundu, P. Adsorption of Congo Red Dye from Aqueous Solutions Using Roots of *Eichhornia crassipes*: Kinetic and Equilibrium Studies. *Energy Procedia* **2014**, *50*, 862–869. [CrossRef]
38. Hu, Z.; Chen, H.; Ji, F.; Yuan, S. Removal of Congo Red from Aqueous Solution by Cattail Root. *J. Hazard. Mater.* **2010**, *173*, 292–297. [CrossRef] [PubMed]
39. Abu-El-Halawa, R.; Zabin, S.A.; Abu-Sittah, H.H. Investigation of Methylene Blue Dye Adsorption from Polluted Water Using Oleander Plant (*Al Defla*) Tissues as Sorbent. *Am. J. Environ. Sci.* **2016**, *12*, 213–224. [CrossRef]
40. Crini, G.; Peindy, H.N.; Gimbert, F.; Robert, C. Removal of C.I. Basic Green (Malachite Green) from aqueous solutions by adsorption using cyclodextrin-based adsorbent: Kinetic and equilibrium studies. *Sep. Purif. Technol.* **2007**, *53*, 97–110. [CrossRef]
41. Fiol, N.; Villaescusa, I. Determination of sorbent point zero charge:usefulness in sorption studies. *Environ. Chem. Lett.* **2009**, *7*, 79–84. [CrossRef]
42. Chanzu, H.A.; Onyari, J.M.; Shiundu, P.M. Brewers' spent grain in adsorption of aqueous Congo Red and Malachite Green dyes: Batch and continuous flow systems. *J. Hazard. Mater.* **2019**, *380*, 120897. [CrossRef] [PubMed]
43. Li, H.X.; Zhang, R.J.; Tang, L.; Zhang, J.H.; Mao, Z.G. Use of cassava residue for the removal of Congo red from aqueous solution by a novel process incorporating adsorption and in vivo decolorization. *BioResources* **2014**, *9*, 6682–6698. [CrossRef]
44. Jain, R.; Sikawar, S. Adsorption and desorption studies of Congo red using low-costadsorbent: Activated de-oiled mustard. *Desalination Water Treat.* **2013**, *52*, 7400–7411. [CrossRef]
45. Hameed, B.H.; Ahmad, A.A. Batch adsorption of methylene blue from aqueous solution by garlic peel, an agricultural waste biomass. *J. Hazard. Mater.* **2009**, *164*, 870–875. [CrossRef]
46. Bharathi, K.S.; Ramesh, S.T. Removal of dyes using agricultural waste as low-cost adsorbents: A review. *Appl. Water Sci.* **2013**, *3*, 773–790. [CrossRef]
47. Langmuir, I. The adsorption of gases on plane surfaces of glass, mica and platinum. *J. Am. Chem. Soc.* **1918**, *40*, 1361–1403. [CrossRef]
48. Freundlich, H.M.F. Over the Adsorption in Solution. *J. Phys. Chem.* **1906**, *57*, 385–471.
49. Sadaf, S.; Bhatti, H.N.; Nausheen, S.; Noreen, S. Potential Use of Low-Cost Lignocellulosic Waste for the Removal of Direct Violet 51 from Aqueous Solution: Equilibrium and Breakthrough Studies. *Arch. Environ. Contam. Toxicol.* **2014**, *66*, 557–571. [CrossRef] [PubMed]
50. Gupta, S.S.; Bhattacharyya, K.G. Kinetics of adsorption of metal ions on inorganic materials: A review. *Adv. Colloid Interface Sci.* **2011**, *162*, 39–58. [CrossRef] [PubMed]
51. Lagergren, S. About the theory of so-called adsorption of soluble substances, Zur theorie der sogenannten adsorption gel?ster stoffe. *Kungliga Svenska Vetenskapsakademiens Handlingar Band* **1898**, *24*, 1–39.

52. Ali, R.M.; Hamad, H.A.; Hussein, M.M.; Malash, G.F. Potential of using green adsorbent of heavy metal removal from aqueous solutions: Adsorption kinetics, isotherm, thermodynamic, mechanism and economic analysis. *Ecol. Eng.* **2016**, *91*, 317–332. [CrossRef]
53. Ho, Y.S.; McKay, G. Sorption of dye from aqueous solution by peat. *Chem. Eng. J.* **1998**, *70*, 115–124. [CrossRef]
54. Pap, S.; Radonić, J.; Trifunović, S.; Adamović, D.; Mihajlović, I.; Vojinović Miloradov, M.; Turk Sekulić, M. Evaluation of the adsorption potential of eco-friendly activated carbon prepared from cherry kernels for the removal of Pb^{2+}, Cd^{2+} and Ni^{2+} from aqueous wastes. *J. Environ. Manag.* **2016**, *184*, 297–306. [CrossRef]
55. Ojedokun, A.T.; Bello, O.S. Kinetic modeling of liquid-phase adsorption of Congo red dye using guava leaf-based activated carbon. *Appl. Water Sci.* **2017**, *7*, 1965–1977. [CrossRef]
56. Olgun, A.; Atar, N.; Wang, S. Batch and column studies of phosphate and nitrate removal adsorption on waste solids containing boron impurity. *Chem. Eng. J.* **2013**, *222*, 108–119. [CrossRef]
57. Weber, W.J.; Morris, J.C. Advances in water pollution research: Removal of biologically resistant pollutant from wastewater by adsorption. In Proceedings of the International Conference on Water Pollution Symposium 2, London, UK, 3–7 September 1962; Pergamon: Oxford, UK, 1962; pp. 231–266.